

Photothermal-Contrast Method Based on *In Situ* Gold Nanostructure Formation for Phenylalanine Detection in Human Blood

Ludovica Maugeri, Maria Anna Messina, Martino Ruggieri, and Salvatore Petralia*

Cite This: <https://doi.org/10.1021/acsanm.3c02651>

Read Online

ACCESS |



Metrics & More



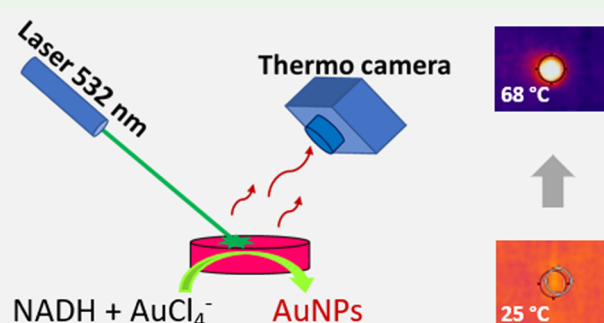
Article Recommendations



Supporting Information

ABSTRACT: An innovative approach based on photothermal contrast to enhance analytical sensitivity of enzymatic phenylalanine detection at a solid surface was demonstrated. Gold nanoparticles *in situ* produced by the reduced form of nicotinamide adenine dinucleotide, which is generated by an enzymatic reaction, exhibit an excellent photothermal effect upon green-light stimuli. The enzymatic reaction and the nanoparticles process formation were optically investigated. A sensing range of 10–1000 μM with a detection limit of 3.6 μM for phenylalanine detection were demonstrated. The testing with blood samples collected from phenylketonuria patients together with concurrent comparison through tandem mass spectrometry have confirmed the good analytical performances and the robustness and utility of the proposed photothermal-contrast approach for further integration on clinical devices.

KEYWORDS: Phenylalanine, photothermal contrast, gold nanoparticles, Enzymatic reaction, phenylketonuria



their application in biosensing areas,¹² biomedicine,¹³ gene delivery,¹⁴ and lateral flow immunoassay¹⁵ as well as photothermal-induced reactions.¹⁶ The photothermal effect is the most intriguing property of plasmonic nanostructures. Upon irradiation, electrons from the metal nanostructure surface are excited to the conduction band, generating the localized surface plasmon resonance band (LSPR). Then, on the time scale of 100 ps to 1 ns, the photoexcited energy is transferred to the metallic lattice through electron–phonon collisions. This relaxation step induces thermal dissipation and releases the thermal energy to the surrounding medium.¹⁷

The ability to rapidly recognize biomolecules in human fluids enables self-monitoring and improves outcomes. This opportunity has increased the diffusion of point-of-care devices able to perform easy and low-cost molecular detection. In this scenario, the development of an integrated platform for diagnostic and therapy monitoring has recently increased its diffusion.^{1–5} Phenylketonuria (PKU) is the most common amino acid disorder, caused by impairment of the enzyme phenylalanine hydroxylase, which converts phenylalanine (Phe) to tyrosine (Tyr). As a consequence of the enzymatic rest, PKU patients store high levels of Phe, which become very toxic for the central nervous system. Phe is an amino acid making up proteins found in many foods, so PKU patients are forced to follow a severe diet-therapy to limit the Phe intake. The compliance with the diet is monitored through the evaluation of Phe levels in blood. Therefore, the regularly lifelong monitoring of the Phe concentration is crucial for the patient's well-being.^{6–8} Recently various analytical approaches for the detection of Phe have been developed. They include a nonenzymatic method based on recognition of Phe by interaction with specific DNA-aptamers sequences,⁹ enzymatic approaches mainly based on phenylalanine ammonia lyase enzyme (PAL)¹⁰ and on phenylalanine dehydrogenase enzyme (PDH) assisted by redox or colorimetric mediators.¹¹

Great efforts have been made in the development of nanostructured materials to improve analytical performance and enable the integration of assays into miniaturized sensing devices. In this scenario, optical, electrical, physical, and photothermal properties of nanostructured materials enable

In the photothermal-contrast approach, the energy light absorbed by materials is converted into heat, which is released to the surroundings creating a thermal lens recorded by the thermocamera. This effect could be improved by various nanostructured materials. Among these, gold nanoparticles, due to their easy synthesis, high stability, and good biocompatibility, are the most diffuse nanomaterials used for photothermal application including the integration on paper-based biosensors.¹⁸ Herein, we report an innovative approach based on photothermal contrast to improve sensitivity of

Received: June 12, 2023

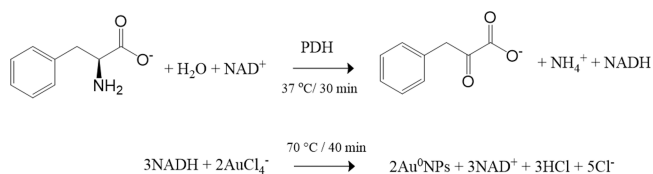
Accepted: July 6, 2023

enzymatic reactions through the heat generated by metallic nanoparticles upon light stimulation.

The amount of heat generated by metallic nanoparticles can be described by the equation $Q = N \times C_{\text{abs}} \times I$, where the total heat generation (Q , Wm^3) is the combined contribution of the metallic nanoparticles amount (N , NPsm^{-3}), metallic nanoparticles absorption cross-section (C_{abs} , m^2), and source laser density (I , Wm^2).¹⁹

The enzymatic conversion of Phe through the enzyme phenylalanine dehydrogenase, followed by the *in situ* gold nanoparticle formation, has been selected as a model to assess the photothermal-contrast performances (Scheme 1).

Scheme 1. Schematic Sensing Strategy



In detail, the first mechanism depicted in Scheme 1 consists of the specific conversion of phenylalanine to phenylpyruvate, catalyzed by the enzyme PDH in the presence of a NAD⁺ cofactor (reaction 1). The neo-formed nicotinamide adenine dinucleotide (NADH) was spectroscopically confirmed through the appearance of the absorption band around 340 nm. Next, the second step involves electron transfer from NADH to Au³⁺ to produce *in situ* spherical gold nanoparticles (reaction 2). Both reactions were spectroscopically monitored in the wavelength range of 250–1000 nm. In particular, Figure 1A illustrates the formation of the absorption band at around 340 nm to indicate the formation of NADH by reaction 1. The Phe concentration range investigated from 10 to 1000 μM was according to the European guidelines on phenylketonuria.^{20,21} The absorbance arises with the increase of the Phe amount (0, 10, 20, 100, 500, and 1000 μM). Then, the *in situ* gold nanoparticle formation by reaction 2 was corroborated by the optical absorption changes reported in Figure 1B where the formation of the intense LSPR band centered at 530 nm is evident (Figure 1B). The formation of gold nanoparticles (size about 12 ± 2 nm) was confirmed by TEM investigation, as shown in Figure 1C.

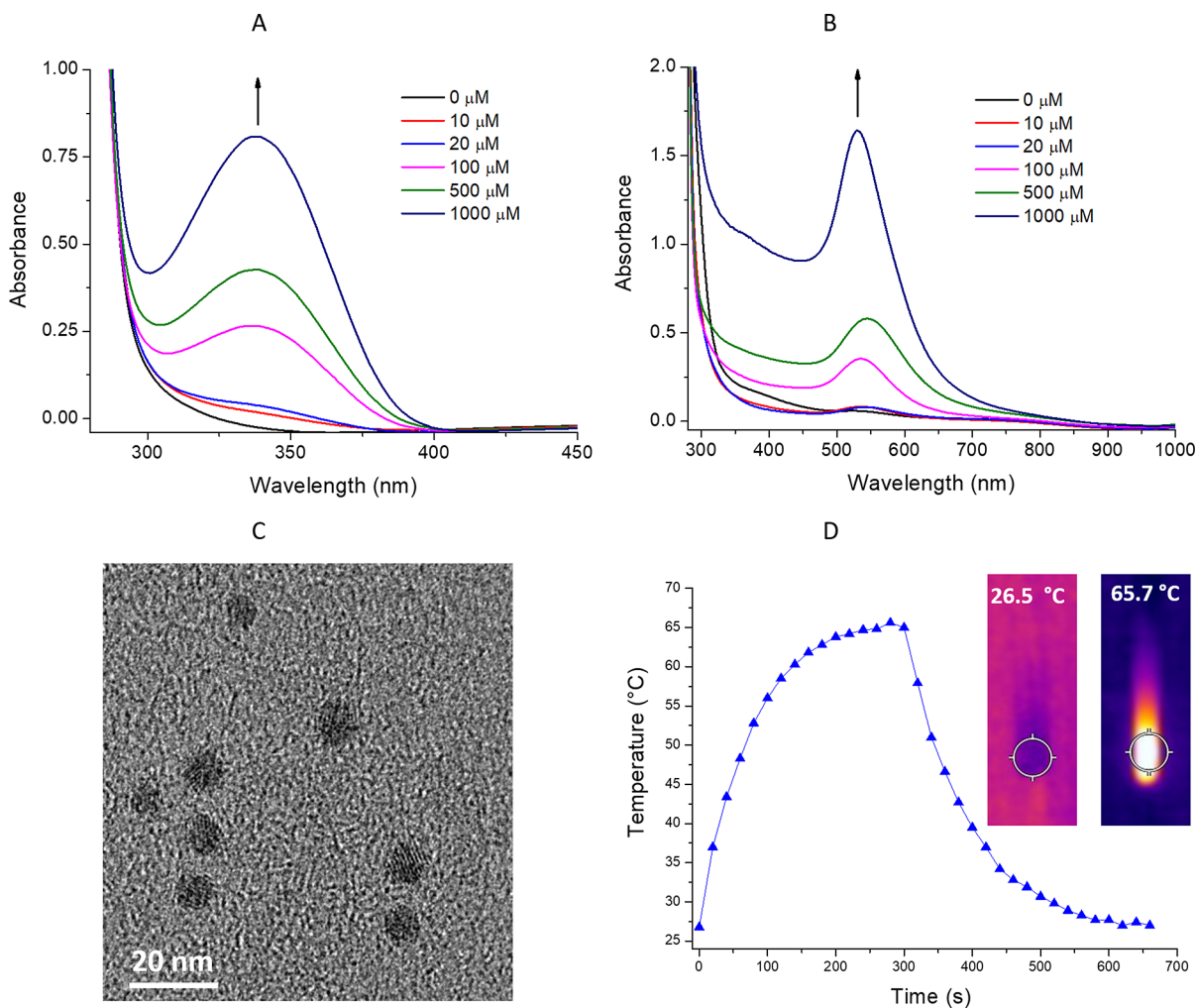


Figure 1. Enzymatic-colorimetric reactions and AuNP characterization: (A) Optical absorption spectra changes for enzymatic reaction 1 in solution (the appearance of absorption band at around 340 nm indicates the NADH formation). (B) Optical absorption spectra changes for gold nanoparticle process formation (reaction 2) in solution. (C) Representative TEM image of AuNPs formed by reactions 1 and 2 in solution. (D) Photothermal cycle for AuNPs upon light irradiation (Phe concentration = 1 mM, $\text{Abs}_{532\text{ nm}} = 1.6$, laser excitation wavelength = 532 nm, power = 200 mW, volume = 100 μL). Insets represent thermographs of AuNPs before (26.5 $^\circ\text{C}$) and after (65.7 $^\circ\text{C}$) green-light excitation.

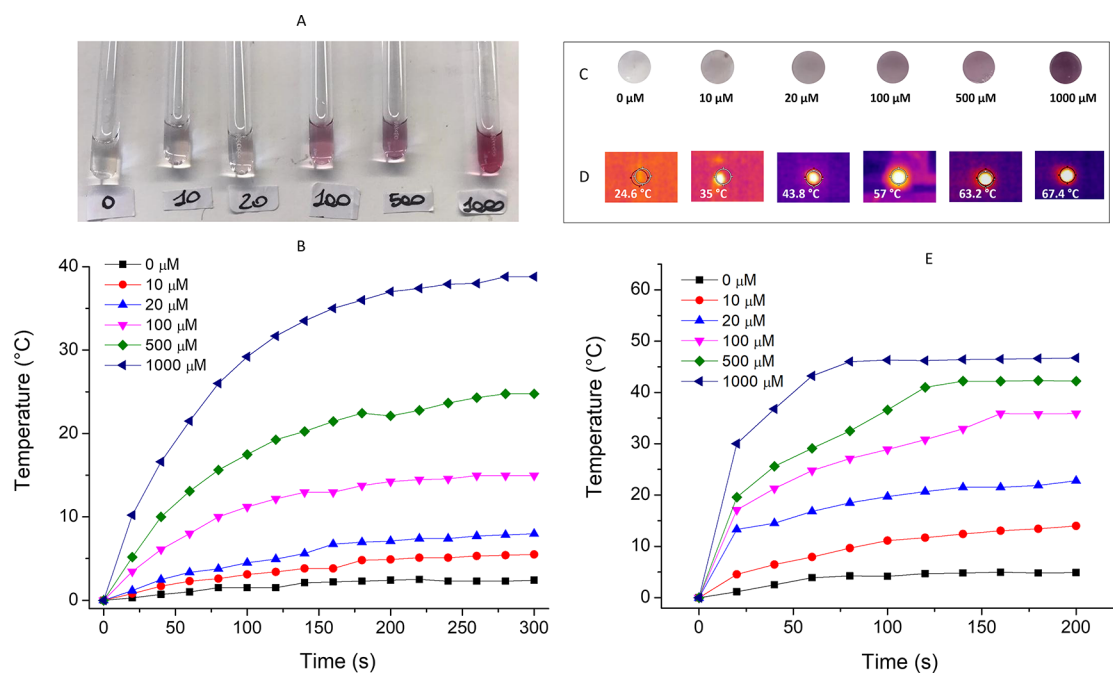


Figure 2. Photothermal experiments for enzymatic-colorimetric reactions at different Phe amounts (0, 10, 20, 100, 500, and 1000 μM): (A) Representative photograph of aqueous dispersion AuNPs into the photothermal holder. (B) Photothermal effect generated from AuNPs formed in aqueous dispersion (sample volume 100 μL) at different Phe amount. (C) Representative photographs and (D) thermography of AuNPs formed at membrane surface at different Phe amount. (E) Photothermal effect generated from AuNPs formed at membrane surface at various Phe amounts.

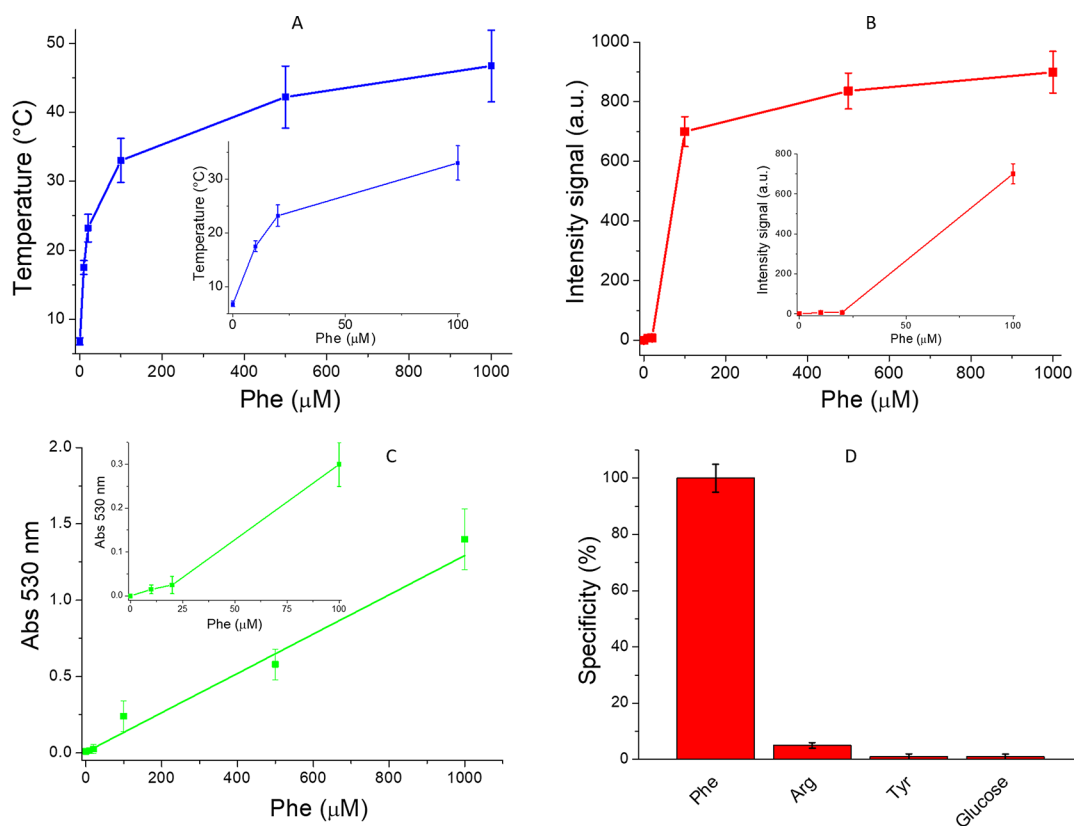


Figure 3. Analytical performances comparison for different Phe concentrations (0, 10, 20, 100, 500, and 1000 μM) and selectivity test: (A) Photothermal-contrast response after 120 s of irradiation time. (B) Optical-contrast response. (C) Optical density response. (D) Specificity (%) of the photothermal-contrast method versus different biomolecules.

Since AuNPs show an intense LSPR absorption band in the region of 500–600 nm, as expected, they exhibit excellent photothermal conversion upon photoexcitation (laser source

532 nm). Figure 1D reports the temperature changes, monitored by a thermocamera, for an aqueous dispersion of AuNPs formed through the reactions in Scheme 1. A net increase of temperature

of about 40 °C in 300 s was observed during laser stimulus (heating process). As the laser is switched off, the temperature decreases, reaching the environment temperature (cooling process).

Additionally, our findings show an undoubted photothermal effect dependent on the amount of AuNPs, which is related to the starting Phe concentration. Figure 2A and B reports the photothermal effect for AuNPs formed in solution and at the membrane surface, respectively, using different amounts of Phe (0, 10, 20, 100, 500, and 1000 μM) and according to the reactions reported in Scheme 1.

In detail, Figure 2A illustrates the aqueous dispersion AuNP samples on a photothermal glass tube holder (volume 100 μL). It is evident as the typical gold nanoparticle color becomes more intense as the Phe quantity increase. Photothermal investigations shown a negligible increase of temperature (about 2.1 °C) for the reference sample (Phe 0 μM). Whereas a net increase of photothermal temperature to 5.6, 7.8, 14.9, 24.7, and 38.9 °C was observed as the Phe amount rose from 10, 20, 100, 500, to 1000 μM (Figure 2B).

To demonstrate the AuNP photothermal effect at the solid surface and to assess the photothermal-contrast efficiency, both reactions 1 and 2 were performed at the nitrocellulose surface using different Phe concentrations, as described in the experimental section. The purple-colored membrane clearly indicates the effectiveness of the *in situ* AuNP process formation (Figure 2C).

The photothermal-contrast testing was performed by irradiating the membrane surface with a green-light source (laser 532 nm, power 0.2W) and capturing the thermographs of the membrane after each 20 s (Figure 2D). Similarly, to the previous test, a slight increase of temperature (about 4.8 °C) for the reference sample (Phe 0 μM) was observed, whereas the temperature increases to 11.2, 22.8, 35.9, 42.2, and 46.7 °C as the Phe amount increases from 10, 20, 100, 500 to 1000 μM , as depicted in Figure 2E. These data confirm that the photothermal effect generated by AuNPs is quantitatively related to the starting Phe concentration as well this effect can be easily and efficiently monitored at a solid surface by a standard thermocamera.

An interesting comparison between the proposed photothermal-contrast approach with optical contrast^a and the standard optical-density approach was performed.

The photothermal-contrast approach showed a nonlinear response^b for the detection of Phe concentration from 10 to 1000 μM at a solid surface (Figure 3A). The limit of detection (LoD) calculated as $3 \times \sigma_{\text{background}}$ (where $\sigma_{\text{background}} = 1.2$ is the standard deviation of background) was about 3.6 μM , and the limit of quantification (LoQ) calculated as $9 \times \sigma_{\text{background}}$ was about 10.8 μM . Similarly, a nonlinear response was observed for the same samples investigated by the optical-contrast mode (Figure 3B). In this case, lower LoD (39.6 μM ; $\sigma_{\text{background}} = 13.2$) and LoQ (118 μM) were observed. While as expected, the spectroscopically standard optical-density method showed a linear response for a Phe concentration range of 10–1000 μM in solution ($Y = 0.0015 + X0.001$; $R^2 = 0.9907$) with a LoD of about 0.1 μM and LoQ of about 0.9 μM (Figure 3C). These comparison data indicate that the proposed photothermal-contrast approach is a suitable analytical method for the detection and quantification of Phe in PKU disease, where the Phe amounts are acceptable in the range of 50–360 and are abnormal for values above 360 μM .^{20,21} Moreover, this method based on photothermal measurement at the membrane surface is

very versatile and could be integrated in a miniaturized and portable device. Contrarily, although the standard optical-density method has very high sensitivity in terms of LoD and LoQ, it is too hard to integrate in a miniaturized device. While the optical-contrast approach can be easily integrated in a paper-based device, the analytical performances are not enough to be used for the Phe monitoring in PKU disease.

Moreover, the capability of the assay to selectively discriminate between Phe versus other molecules such as arginine, tyrosine at a concentration of 200 μM , and glucose at a concentration of 5 mM was investigated. The data reported in Figure 3D confirm the high specificity of the proposed assay for the recognition of Phe. Our results show excellent sensitivity and good specificity performances for Phe recognition at a solid surface using a photothermal-contrast approach, according to the literature data.¹⁵

The higher performance of the photothermal-contrast approach, with respect to the optical contrast, is related to the high photothermal signal-to-noise ratio value. In the photothermal method, the signal-to-noise ratio could be improved by different approaches such as a better thermal isolation from the surface and enhancing the absorption cross section of materials as demonstrated by single molecule detection reported in literature.²² Contrarily, surface roughness, slight variations in the refraction index of the sample, and a small absorption cross section decrease the signal-to-noise ratio for the optical-contrast approach.

In order to assess the capability of the proposed photothermal-contrast assay to measure the Phe concentration in human specimens, a vertical flow system (VFS) was designed and prepared. The VFS is composed of (1) a blood filter membrane (diameter 8 mm) for plasma filtration, (2) an enzymatic layer composed by agarose 0.4% with all reagents embedded for enzymatic reaction 1, and (3) a photothermal contrast nitrocellulose membrane containing all reagents for AuNP formation (reaction 2) (Figure 4A). These components are housed on a cylindrical holder for easy handling.

The amount of Phe in filtered plasma was measured through the photothermal effect generated by AuNPs produced by reactions 1 and 2 at the membrane surface. A small volume of Au seeds was used to improve the nanoparticle formation as detailed in the Supporting Information. The temperature

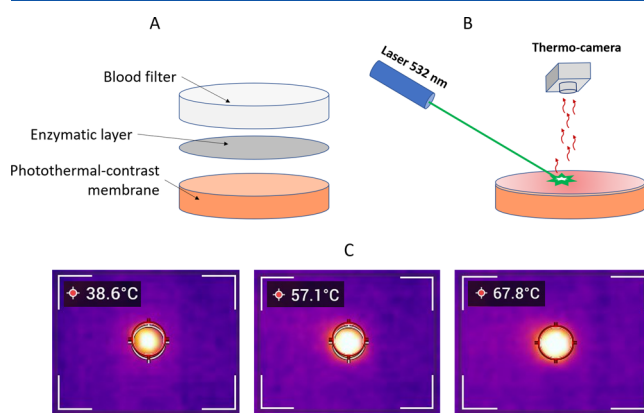


Figure 4. Photothermal-contrast experiments with human samples: (A) Schematics of vertical flow system. (B) Photothermal-contrast readout setup, (C) Representative thermographs of membrane for photothermal-contrast experiments on VFS.

recorded at the membrane surface by the thermocamera was related to the Phe amount in a blood sample (Figure 4B).

Human blood samples were used for the experiments. In particular, two samples were collected from PKU patients (PKU1 and PKU2) and a sample from the healthy control (HC1). For comparison, the Phe amount was measured by a tandem-MS technique obtaining for PKU1 a Phe concentration value of 148 μM , for PKU2 a Phe concentration value 916 μM , and an HC1 concentration value of 38 μM . Each experiment was replicated three times (Figure S1).

In detail, an amount of fresh whole blood (volume 20 μL) was placed on a blood filter, and after 3 min of filtration, a volume of approximately 12 μL of a plasma sample was collected by an enzymatic layer. The filter was removed, and the VFS was incubated at 37 $^{\circ}\text{C}$ for 30 min and 70 $^{\circ}\text{C}$ for 50 min (Figure S2). Then, thermographs were captured during green-light irradiation (laser 532 nm, power 200 mW). The temperatures recorded after 120 s of irradiation were 38.6 $^{\circ}\text{C}$ for the reference HC1, 57.1 $^{\circ}\text{C}$ for the PKU1 sample, and 67.8 $^{\circ}\text{C}$ for the PKU2 sample (Figure 4C). The environment temperature recorded was about 22 $^{\circ}\text{C}$. The Phe concentrations for the investigated samples were calculated by interpolation with the curve reported in Figure 3A. In particular, a Phe concentration of $20 \pm 5 \mu\text{M}$ was obtained for HC1 (38 μM), a Phe concentration of $157 \pm 15 \mu\text{M}$ for PKU1 (148 μM), and a Phe concentration of $946 \pm 50 \mu\text{M}$ for PKU2 (916 μM). These data well corroborate with the Phe concentration values obtained by tandem-MS techniques. Combining the high specificity of the enzyme recognition with the excellent sensitivity of the photothermal contrast approach,^{22,23} an unprecedented and innovative enzymatic-photothermal assay for phenylalanine detection at a solid surface was developed. Supported by the commercially available equipment, properly designed and produced for photothermal-contrast measurements,²⁴ further research activities will be focused on the development of a biosensor system based on the proposed approach.

In conclusion, a novel photothermal-contrast method based on *in situ* gold nanoparticle formation at the membrane surface was demonstrated. The enzymatic reaction and nanoparticles process formation were optically investigated. Photothermal properties and the nanosized dimension for gold nanoparticles were confirmed. Successful recognition of Phe in blood samples from PKU patients was proven, together with the integration of the assay on miniaturized vertical flow systems. With further modifications of the method, such as light source and nanoparticle shape and size as well membrane substrate, additional improvement in performance as a larger dynamic range and higher sensitivity can be expected. This approach properly integrated in a miniaturized system could enable the self-monitoring of Phe reducing cost and time analysis. Thus, we can conclude that the proposed photothermal contrast assay based on *in situ* AuNP formation is a promising detection mode for improving the development of a portable and cost-effective biosensing system.

■ ASSOCIATED CONTENT

SI Supporting Information

The Supporting Information is available free of charge at <https://pubs.acs.org/doi/10.1021/acsanm.3c02651>.

Enzymatic reaction procedure, photothermal experiments, vertical flow system preparation, human recruit-

ment, photodetector reader, and tandem-mass analysis. (PDF)

■ AUTHOR INFORMATION

Corresponding Author

Salvatore Petralia – Department of Drug and Health Sciences, University of Catania, 95125 Catania, Italy; orcid.org/0000-0001-5692-1130; Email: salvatore.petralia@unict.it

Authors

Ludovica Maugeri – Department of Drug and Health Sciences, University of Catania, 95125 Catania, Italy; orcid.org/0000-0003-3839-3754

Maria Anna Messina – Expanded Newborn Screening Laboratory, A.O.U Policlinico “G. Rodolico San Marco”, 95125 Catania, Italy

Martino Ruggieri – Expanded Newborn Screening Laboratory, A.O.U Policlinico “G. Rodolico San Marco”, 95125 Catania, Italy; Unit of Clinical Pediatrics, Department of Clinical and Experimental Medicine, University of Catania, 95125 Catania, Italy

Complete contact information is available at: <https://pubs.acs.org/10.1021/acsanm.3c02651>

Author Contributions

The manuscript was written through contributions of all authors. All authors have given approval to the final version of the manuscript.

Author Contributions

L. Maugeri and M. A. Messina equally contributed.

Funding

This research was supported by PKU Smart Sensor” project, funded under Action 1.1.5 POR FESR 2014-2020, CUP G89J18000710007.

Notes

The authors declare no competing financial interest.

■ ABBREVIATIONS

PKU = Phenylketonuria
Phe = Phenylalanine
VFS = Vertical flow system

■ ADDITIONAL NOTES

^aIn optical contrast, the reflectance signals at the surface level are measured by a LED/photodetector system. The optical-contrast signal is the difference in light intensity (absorption, emission, reflectance) between the image and the background.

^bThe nonlinear fitting equation is $Y = Y_0 + A^{R_0 * X}$, ($Y_0 = 38.8 \pm 3.5$, $A = -31.9 \pm 3.5$, and $R_0 = -0.038 \pm 0.008$).

■ REFERENCES

- (1) Tehrani, F.; Teymourian, H.; Wuerstle, B.; et al. An integrated wearable microneedle array for the continuous monitoring of multiple biomarkers in interstitial fluid. *Nat. Biomed. Eng.* **2022**, *6*, 1214.
- (2) Wang, M.; Yang, Y.; Min, J.; et al. A wearable electrochemical biosensor for the monitoring of metabolites and nutrients. *Nat. Biomed. Eng.* **2022**, *6*, 1225.
- (3) Rink, S.; Baeumner, A. J. Progression of Paper-Based Point-of-Care Testing toward Being an Indispensable Diagnostic Tool in Future Healthcare. *Anal. Chem.* **2023**, *95*, 1785.
- (4) Petralia, S.; Conoci, S. PCR Technologies for Point of Care Testing: Progress and Perspectives. *ACS sensors* **2017**, *2*, 876.

- (5) Christodouleas, D. C.; Kaur, B.; Chorti, P. From point-of-care testing to eHealth diagnostic devices (eDiagnostic). *ACS Cent. Sci.* **2018**, *4*, 1600.
- (6) Baird, S.; Clinton Frazee, C.; Garg, U. Quantification of 25-Hydroxyvitamin D2 and D3 Using Liquid Chromatography-Tandem Mass Spectrometry. *Methods in Molecular Biology* **2022**, *2546*, 391.
- (7) van Wegberg, A. M. J.; MacDonald, A.; Ahring, K.; Belanger-Quintana, A.; Blau, N.; Bosch, A. M.; Burlina, A.; Campistol, J.; Feillet, F.; Gizewska, M.; Huijbregts, S. C.; Kearney, S.; Leuzzi, V.; Maillot, F.; Muntau, A. C.; van Rijn, M.; Trefz, F.; Walter, J. H.; van Spronsen, F. J. The complete European guidelines on phenylketonuria: diagnosis and treatment. *Orphanet J. Rare Dis* **2017**, *12*, 162.
- (8) Biasucci, G.; Brodosi, L.; Bettocchi, I.; Noto, D.; Pochiero, F.; Urban, M. L.; Burlina, A. The management of transitional care of patients affected by phenylketonuria in Italy: Review and expert opinion. *Mol. Genet. Metab.* **2022**, *136*, 94.
- (9) Yang, J.; Bi, Q.; Song, X. B.; Yuan, R.; Xiang, Y. Aptamer/organometallic receptor-based and label-free sensitive electrochemical detection of amino acid via multi-pedal DNA walker/DNAzyme amplifications. *Sens. and Act. B: Chem.* **2023**, *375*, 132876.
- (10) Messina, M. A.; Meli, C.; Conoci, S.; Petralia, S. A facile method for urinary phenylalanine measurement on paper-based lab-on-chip for PKU therapy monitoring. *Analyst* **2017**, *142*, 4629.
- (11) Messina, M. A.; Maugeri, L.; Forte, G.; Ruggieri, M.; Petralia, S. A highly sensitive colorimetric approach based on tris (bipyridine) Ruthenium (II/III) mediator for the enzymatic detection of phenylalanine. *Front. Chem.* **2023**, *11*, 1164014.
- (12) Parolo, C.; Merkoçi, A. Paper-based nanobiosensors for diagnostics. *Chem. Soc. Rev.* **2013**, *42*, 450.
- (13) Consoli, G. M. L.; Forte, G.; Maugeri, L.; Consoli, V.; Sorrenti, V.; Vanella, L.; Buscarino, G.; Agnello, S.; Camarda, M.; Granata, G.; Ferreri, L.; Petralia, S. Near-Infrared-Responsive Choline-Calix[4]-arene-Gold Nanostructures for Potential Photothermal. *ACS Appl. Nano Mater.* **2023**, *6*, 358.
- (14) Petralia, S.; Forte, G.; Aiello, M.; Nocito, G.; Conoci, S. Photothermal-triggered system for oligonucleotides delivery from cationic gold nanorods surface: A molecular dynamic investigation. *Coll. and Surf. B: Biointer.* **2021**, *201*, 111654.
- (15) Qin, W.; Chan, Boulware, D. R.; Akkin, T.; Butler, E. K.; Bischof, J. C. Significantly Improved Analytical Sensitivity of Lateral Flow Immunoassays by Thermal Contrast. *Angew. Chem.* **2012**, *51*, 4358.
- (16) Maugeri, L.; Forte, G.; Messina, M. A.; Camarda, M.; Ventimiglia, G.; Consoli, G. M. L.; Petralia, S. Photochemical Synthesis of β -Cyclodextrin/Cobalt Oxide Nanoparticles as Photothermal Agents for Photothermal-Induced Enzymatic Reaction. *ACS Appl. Nano Mater.* **2022**, *5*, 10167.
- (17) Kim, M.; Lee, J.-H.; Nam, J.-M. Plasmonic Photothermal Nanoparticles for Biomedical Applications. *Adv. Sci.* **2019**, *6*, 1900471.
- (18) Quesada-González, D.; Merkoçi, A. Nanoparticle-based lateral flow biosensors. *Biosens. Bioelectron.* **2015**, *73*, 47.
- (19) Qin, Z.; Bischof, J. C. Thermophysical and biological responses of gold nanoparticle laser heating. *Chem. Soc. Rev.* **2012**, *41*, 1191.
- (20) van Wegberg, A. M. J.; MacDonald, A.; Ahring, K.; Belanger-Quintana, A.; Blau, N.; Bosch, A. M.; Burlina, A.; Campistol, J.; Feillet, F.; Gizewska, M.; Huijbregts, S. C.; Kearney, S.; Leuzzi, V.; Maillot, F.; Muntau, A. C.; van Rijn, M.; Trefz, F.; Walter, J. H.; van Spronsen, F. J. The complete European guidelines on phenylketonuria: diagnosis and treatment. *Orphanet Journal of Rare Diseases* **2017**, *12*, 162.
- (21) van Spronsen, F. J.; van Wegberg, A. M.; Ahring, K.; Belanger-Quintana, A.; Blau, N.; Bosch, A. M.; Burlina, A.; Campistol, J.; Feillet, F.; Gizewska, M.; Huijbregts, S. C.; Kearney, S.; Leuzzi, V.; Maillot, F.; Muntau, A. C.; Trefz, F. K.; van Rijn, M.; Walter, J. H.; MacDonald, A. Key European guidelines for the diagnosis and management of patients with phenylketonuria. *Lancet Diabetes Endocrinol* **2017**, *5*, 746–756.
- (22) Gaiduk, A.; Yorulmaz, M.; Ruijgrok, P. V.; Orrit, M. Room-temperature detection of a single molecule's absorption by photothermal contrast. *Science* **2010**, *330*, 353–356.
- (23) Kim, M.; Lee, J.-H.; Nam, J.-M. Plasmonic Photothermal Nanoparticles for Biomedical Applications. *Advanced Science* **2019**, *6*, 1900471.
- (24) Calorsito VIS-NIR. *NanoLockin*. <https://www.nanolockin.com/products/calorsito-vis-nir>.